AIP | The Journal of Chemical Physics

High-pressure vibrational properties of polyethylene

Luca Fontana, Mario Santoro, Roberto Bini, Diep Q. Vinh, and Sandro Scandolo

Citation: J. Chem. Phys. **133**, 204502 (2010); doi: 10.1063/1.3507251
View online: http://dx.doi.org/10.1063/1.3507251
View Table of Contents: http://jcp.aip.org/resource/1/JCPSA6/v133/i20
Published by the American Institute of Physics.

High-pressure vibrational properties of polyethylene

Luca Fontana,[1] Mario Santoro,[1,2] Roberto Bini,[1,3,a)] Diep Q. Vinh,[4] and Sandro Scandolo[5]
[1]*LENS, European Laboratory for Non-Linear Spectroscopy, Via N. Carrara 1, I-50019 Sesto Fiorentino (FI), Italy*
[2]*IPCF-CNR, c/o Università di Roma "La Sapienza," I-00185 Roma, Italy*
[3]*Dipartimento di Chimica, Università degli Studi di Firenze, Via della Lastruccia 3, I-50019 Sesto Fiorentino (FI), Italy*
[4]*International School for Advanced Studies (SISSA), Via Beirut 2-4, 34014 Trieste, Italy*
[5]*The Abdus Salam International Centre for Theoretical Physics (ICTP) and Democritos CNR-IOM, I-34151 Trieste, Italy*

(Received 15 June 2010; accepted 8 October 2010; published online 24 November 2010)

The pressure evolution of the vibrational spectrum of polyethylene was investigated up to 50 GPa along different isotherms by Fourier-transform infrared and Raman spectroscopy and at 0 K by density-functional theory calculations. The infrared data allow for the detection of the orthorhombic *Pnam* to monoclinic $P2_1/m$ phase transition which is characterized by a strong hysteresis both on compression and decompression experiments. However, an upper and lower boundary for the transition pressure are identified. An even more pronounced hysteresis is observed for the higher-pressure transition to the monoclinic $A2/m$ phase. The hysteresis does not allow in this case the determination of a well defined P-T transition line. The ambient structural properties of polyethylene are fully recovered after compression/decompression cycles indicating that the polymer is structurally and chemically stable up to 50 GPa. A phase diagram of polyethylene up to 50 GPa and 650 K is proposed. Analysis of the pressure evolution of the Davydov splittings and of the anomalous intensification with pressure of the IR active wagging mode provides insight about the nature of the intermolecular interactions in crystalline polyethylene. © *2010 American Institute of Physics*. [doi:10.1063/1.3507251]

I. INTRODUCTION

Polyethylene is one of the most common materials in our daily life and accounts for about 40% of the total volume of world production of plastic materials. Polyethylene is also an outstanding engineering plastic in the ultrahigh molecular weight (UHMW) crystalline form that is characterized by excellent mechanical, chemical, and dielectric properties. In addition, polyethylene is a model system among one-dimensional polymers, particularly for what concerns its vibrational properties.[1] In spite of its various applications under severe stress conditions, for example, as a mechanical component or as a part of different kind of prostheses, the characterization of its structural properties at high pressure was limited to a few (2–3) GPa (Refs. 2 and 3) up to a recent characterization by x-ray diffraction and *ab initio* simulations carried out up to 40 GPa.[4]

Polyethylene crystal exhibits, at ambient conditions, an orthorhombic structure ($Pnam$) with two polymeric chains per unit cell.[5] The compressibility of the crystal is strongly anisotropic being one order of magnitude lower along the chain axis direction with respect to the orthogonal directions.[6] Above 200 °C and 0.3 GPa a partially disordered hexagonal phase has been found between the orthorhombic phase and the liquid state.[2,7–11] In this phase the polymeric chains lose the ordered all-trans conformation characterizing the orthorhombic phase. Crystallization through the hexagonal phase yields high-quality crystals of the orthorhombic phase, whereas gauche defects (chain-folding) are always observed when the fluid is crystallized directly into the orthorhombic phase, leading to the formation of amorphous regions in the crystal.[7–11] When polyethylene is subjected to uniaxial compression the formation of a monoclinic ($A2/m$) phase has been reported.[12] This form is metastable at ambient conditions and converts to the orthorhombic phase upon temperature annealing.[13] The unit cell of the monoclinic phase contains two chains, with skeletal planes parallel to each other but with chains shifted with respect to one another by half of the chain periodicity, along the monoclinic axis. Recently, the structural characterization of crystalline polyethylene has been extended to 40 GPa by a combined x-ray diffraction and *ab initio* calculation study.[4] Orthorhombic polyethylene was observed to transform reversibly above 6 GPa to a monoclinic phase with $P2_1/m$ space group (one chain per unit cell). Above 14–16 GPa another phase transition to a different monoclinic phase was detected. The latter is isostructural ($A2/m$) to the monoclinic metastable phase reported in stressed polymers at ambient conditions. All the transitions are characterized by a large hysteresis and coexistence of all three phases is observed up to about 30 GPa, where the signatures of the orthorhombic $Pnam$ phase vanish. The $A2/m$ monoclinic phase was found to be stable over the $P2_1/m$ upon pressure release until polyethylene crystal converts back to the ambient pressure orthorhombic phase, leading to the conclusion that the orthorhombic $Pnam$ and the monoclinic

a)Author to whom correspondence should be addressed. Electronic mail: roberto.bini@unifi.it.

$A2/m$ structures are the only thermodynamically stable crystal phases.

Vibrational studies at high pressure are also rather limited. The Raman lattice modes were studied up to 4 GPa.[14] The pressure dependence of the frequency separation between the IR active Davydov components of the rocking mode was measured up to 4 GPa.[15] The IR spectrum was also studied up to 13 GPa with particular reference to the interchain interaction-induced activity of the IR inactive C–C stretching mode.[16] The Davydov splitting of both infrared and Raman modes have been computed up to 2.5 GPa and have been used to determine the Gruneisen parameters.[17]

Here we report the results of a combined FTIR, Raman, and density functional theory (DFT) computational study on the pressure evolution of the vibrational spectrum of polyethylene up to 50 GPa and 650 K. A fair agreement with the structural data obtained by x-ray diffraction studies is found. The experimental study, performed along different isotherms, allows the determination of the phase diagram of polyethylene up to 50 GPa.

II. METHODS

UHMW polyethylene from Aldrich ($Mw = 3 \times 10^6 - 6 \times 10^6$, $\rho = 0.94$ g/cm^3) has been employed in all the experiments. Commercial polyethylene is always a mixture of the ordered orthorhombic crystal, amorphous domains, and monoclinic impurities ($A2/m$), the relative amounts depending on the preparation method. UHMW polyethylene was preferred to the high density (HD) and high spectroscopic grade (HSG) polymers because it shows, according to the IR spectra (see Fig. 1),[18] the lowest amount of gauche defects (amorphous material) and monoclinic phase. The powder was loaded without any compressing medium in a membrane DAC equipped with rhenium gaskets and low fluorescence IIa or Ia diamonds, for IR and Raman measurements, respectively. The initial sample dimensions were about 150 μm in diameter and 50 μm thick. After the loading all the samples were found to contain a small amount of the metastable monoclinic phase, beside the dominant orthorhombic component. For this reason, thermal annealing of the sample has been always performed at the beginning of the experiment to reduce as much as possible the amount of the monoclinic phase. Polyethylene was melted at low pressure ($P < 4$ kbar) and then recrystallized through the hexagonal phase (see Fig. 2). In Fig. 2 we show how IR spectroscopy is successfully employed to control the quality of the annealing procedure by monitoring the complete disappearance of the monoclinic bands lying at 716 cm^{-1}, as a shoulder of the orthorhombic low frequency peak, and at 1465 cm^{-1}, between the two orthorhombic peaks. In addition, the remarkable narrowing of the orthorhombic lines points to a high crystal quality as confirmed by XRD experiments.[4] All the data presented in this work refer to the samples produced following this annealing procedure. The sample heating was achieved by an external resistive heater and the temperature was measured by a J thermocouple. The sample pressure was determined by the shift of the ruby fluorescence lines using the calibration of Ref. 19 corrected for the high temperature.[20] IR spectra were measured by a FTIR spectrometer (Bruker IFS 120 HR) suitably modified to allow high-pressure measurements.[21] The instrumental resolution was 1 cm^{-1}. Raman spectra were measured in a quasiback scattering geometry (scattering angle of about 152°) by using the 752.5 nm line of a Kr^+ laser. The scattered light was dispersed by a single stage monochromator (1800 grooves/mm) and analyzed by a CCD detector with a resulting instrumental resolution of 0.4 cm^{-1}.

First-principle calculations were carried out within gradient-corrected[22] density-functional theory, as implemented in the Quantum-ESPRESSO code.[23] The ion–electron interaction was described by ultrasoft pseudopotentials, and electronic wave functions were expanded in a plane-wave basis set with kinetic-energy cutoff of up to 110 Ry. Atomic structures in the *Pnam, P2$_1$/m*, and *A2/m* space groups were relaxed at fixed pressure with a conjugate-gradient method and Brillouin zones were sampled with up to 52 special points. At the local minima, the normal modes of vibration at

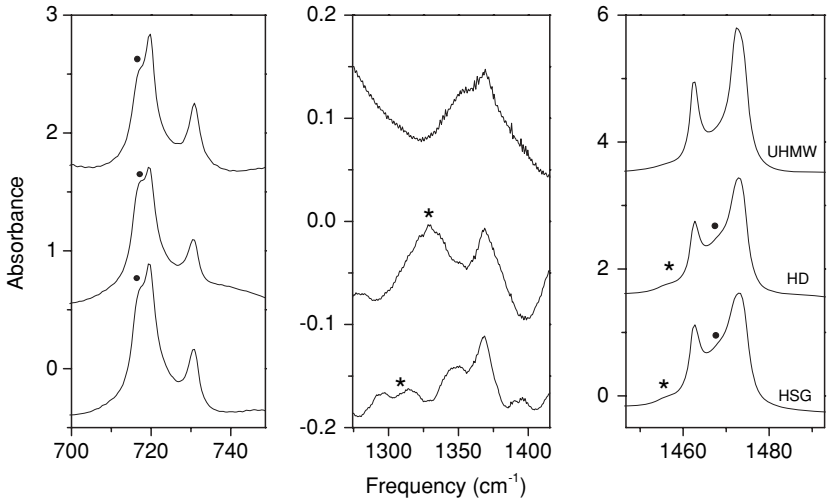

FIG. 1. Infrared spectra of UHMW, HD, and HSG polyethylene. Stars and circles indicate the amorphous and the monoclinic bands of the material, respectively. The other peaks are assigned to the orthorhombic *Pnam* phase.

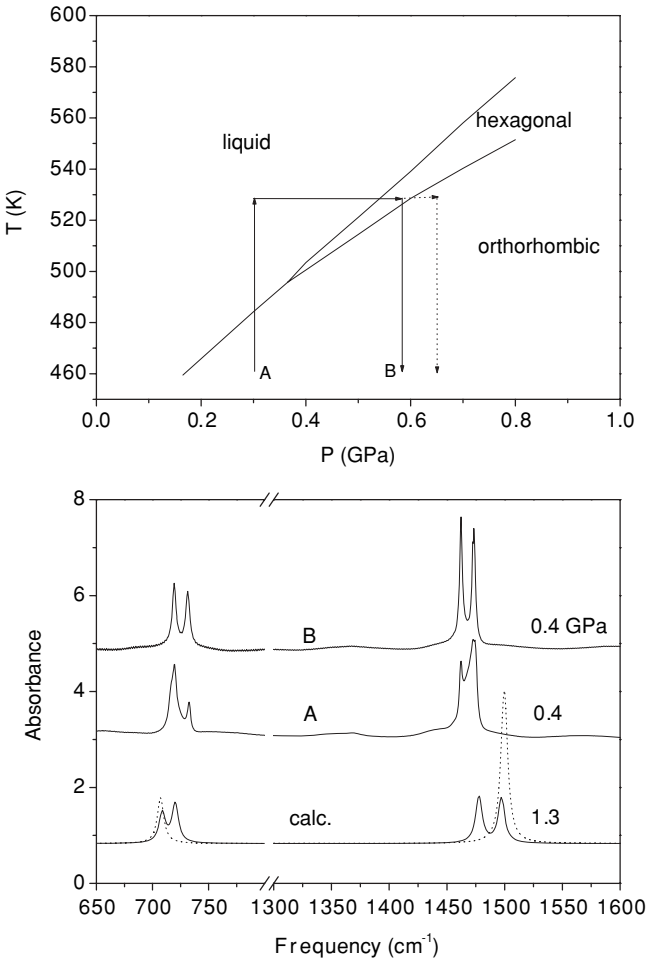

FIG. 2. Upper panel: P–T path followed in the annealing procedure of polyethylene. Lower panel: comparison between the IR spectra measured before (A) and after (B) the annealing procedure and those calculated for the monoclinic $A2/m$ (dashed line) and orthorhombic *Pnam* (full line) phases.

$\Gamma(q=0)$ were calculated by density functional perturbation theory[24] using a norm-conserving pseudopotential with a kinetic-energy cutoff of 80 Ry. Infrared and Raman spectra were also computed using density functional perturbation theory.[24] In particular, the intensities I of the infrared-active modes were obtained as

$$I(\nu) = \sum_{\alpha} \left| \sum_{i} \sum_{\beta} Z^{*}_{i,\alpha\beta} u_{i,\beta}(\nu) \right|^{2}, \quad (1)$$

where $u_{i,\beta}(\nu)$ is the normalized vibrational eigenvector of the atom i in the mode ν. α and β indicate Cartesian directions and $Z^{*}_{i,\alpha\beta}$ is the effective charge tensor of atom i. Raman intensities were obtained using the method described in Ref. 25.

III. RESULTS

According to group theory arguments 14 internal vibrational modes are expected for a single polyethylene chain (point group D_{2h}).[26] Five of them are expected to be active in the IR spectrum, eight in the Raman spectrum, and one inactive in both spectra. The inversion center is preserved in the orthorhombic *Pnam* structure where two polyethylene chains are contained in the unit cell. As a consequence, each vibrational mode splits into two Brillouin zone center components. The atmospheric pressure spectra of the UHMW polyethylene employed in the present study agree nicely with those reported in earlier studies.[27,28] IR and Raman measurements have been performed as a function of pressure along different isotherms. For the sake of clarity the infrared and Raman results will be presented separately.

A. FTIR measurements

We performed different isothermal pressure scans in the 296–625 K temperature range to investigate the phase diagram and to study the chemical stability of the polymer for pressures up to 50 GPa. All the absorption bands were fitted to pseudo-Voigt functions and their frequencies, widths, and intensities analyzed as a function of pressure. There are three regions in the IR spectrum of polyethylene that are commonly employed for crystallinity determination:[18,29] the rocking mode (γ_r) region, which presents in the *Pnam* structure two crystal components at 720 and 731 cm^{-1} (ambient pressure values), the wagging mode (γ_w) at 1176 cm^{-1} extremely weak at ambient conditions, and the two strong crystal components of the scissoring mode (δ) at 1463 and 1473 cm^{-1}. Upon compression several modifications are observed (see Fig. 3). The two components of the rocking mode shift to higher frequency and intensify, but close to the orthorhombic-monoclinic ($P2_1m$) phase transition (P ~ 6 GPa) (Ref. 4) the lower frequency peak remarkably weakens. The low frequency peak of the orthorhombic phase continuously weakens on increasing pressure, vanishing at about 18 GPa, whereas the high frequency component intensifies. This latter peak can be reasonably ascribed to the single Davydov component

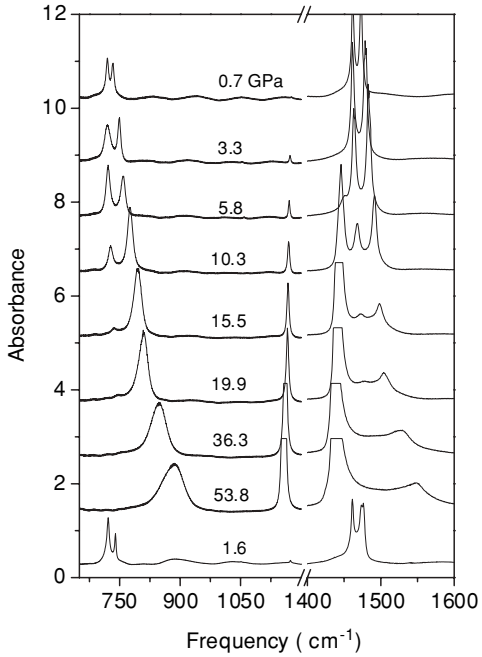

FIG. 3. Selected IR spectra of crystalline polyethylene at 475 K, measured upon pressure increase (from top to bottom) from 0.7 to 53.8 GPa. At the bottom side it is reported the spectrum of the sample measured at the lowest pressure after the complete compression/decompression cycle.

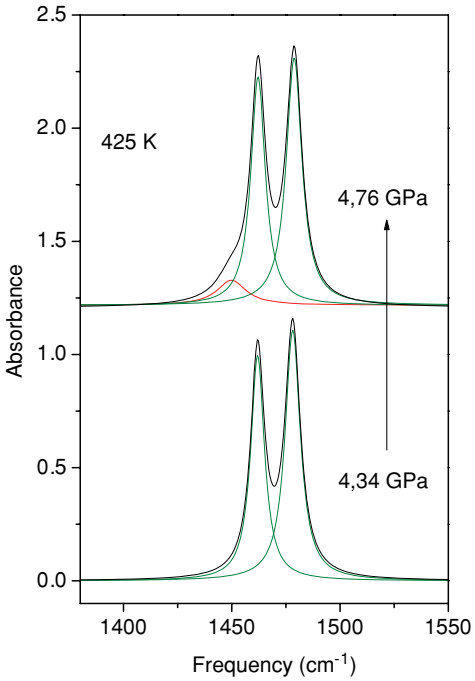

FIG. 4. Decomposition of the IR spectra of crystalline polyethylene measured at 425 K in the scissoring region through the orthorhombic *Pnam* to monoclinic $P2_1m$ transition. The formation of the monoclinic phase is revealed by the appearance of the new peak on the low frequency side of the orthorhombic doublet. The fit was performed with pseudo-Voigt functions.

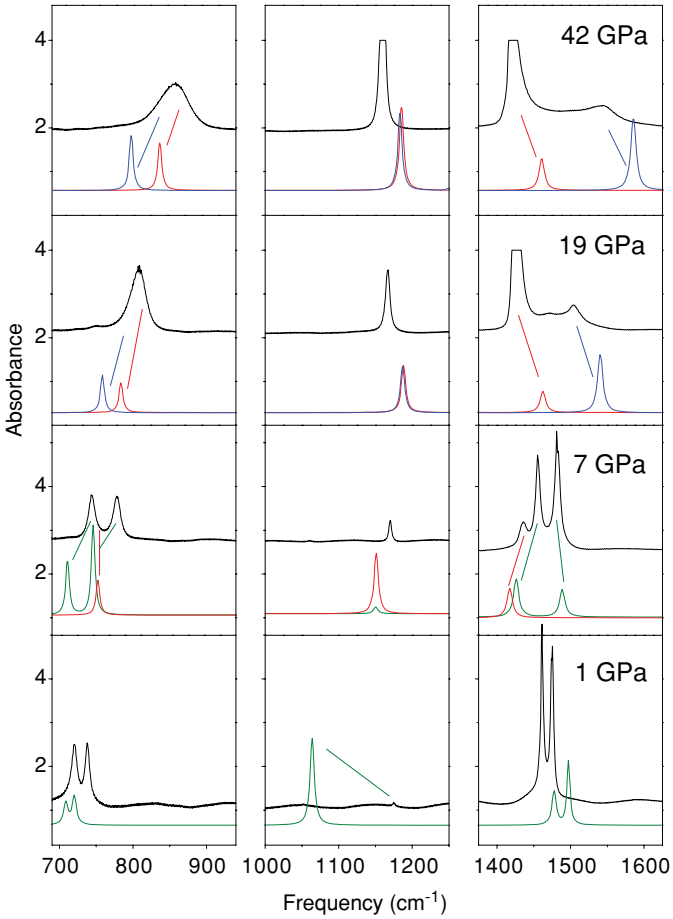

FIG. 5. Comparison between experimental (575 K) and simulated (0 K) infrared spectra at four selected pressures. The calculated spectra are shown with green (orthorhombic *Pnam*), red (monoclinic $P2_1m$), and blue (monoclinic *A2/m*) lines, while the experimental spectra are reported as black lines. Correspondence of the peaks is also indicated. The theoretical bandwidths were fixed to 7 cm^{-1}. The vertical scales of the computed spectra were multiplied by a frequency independent arbitrary factor.

expected for the monoclinic $P2_1m$ phase ($z=1$). The wagging band at 1176 cm^{-1} shows a strong intensification and a softening with increasing pressure. The anomalous intensification of this band, a factor of 15 with respect to the rocking mode going from ambient pressure to 20 GPa, will be discussed later. Finally, another evident spectral change takes place in the scissoring mode region where in correspondence to the *Pnam*-$P2_1m$ phase transition a new peak appears on the low frequency side of the doublet at 1430 cm^{-1} (see Figs. 3 and 4) while, simultaneously, both the components characteristic of the orthorhombic phase remarkably weaken. The new band, assigned to the monoclinic $P2_1m$ phase, greatly intensifies and softens its frequency with rising pressure (Fig. 3).

DFT calculations were able to reproduce some relevant aspects of the pressure evolution of the IR spectrum despite the rather qualitative agreement with the experimental infrared spectra.

The comparison between experimental and simulated spectra is shown in Fig. 5 at four selected pressures. From this comparison it results that only some of the measured absorption bands can be clearly assigned to a single phase. In fact, besides the orthorhombic phase, an unambiguous assignment can be provided only for the strong low frequency peak in the scissoring region (between 1440 and 1450 cm^{-1}) as due to the monoclinic $P2_1m$ phase, and for the monoclinic *A2/m* peak lying between 1500 and 1550 cm^{-1}. Nevertheless, the calculated spectra are extremely useful to explain the complex patterns observed at high pressure as a superposition of spectra relative to the different coexisting phases, as also reported in x-ray diffraction studies.[4] It should be remarked that it is a common feature of DFT calculations to reproduce vibrational frequencies with an accuracy of about 10% which only occasionally reduces to a few percent. The largest discrepancy in our case is obtained for the low-pressure *Pnam* phase, for which DFT errors are expected to be largest, due to the larger inhomogeneity of the charge density distribution.

The IR spectra are completely reversible along the compression–decompression cycle (see Fig. 3) indicating a complete chemical stability of the polymer even under high stress conditions. Nevertheless, a strong hysteresis is revealed. In fact, the monoclinic bands, due to both $P2_1m$ and *A2/m* phases, are indeed observed down to about 3 GPa in substantial agreement with the XRD results.[4]

B. Raman measurements

The orthorhombic and monoclinic crystal phases of polyethylene are characterized by the existence of an inversion symmetry thus making IR and Raman spectra complementary. The pressure evolution of the Raman spectrum was monitored along two isothermal runs at 475 K up to 40 GPa, and at 575 K up to 10 GPa. The observed Raman peaks were fitted to pseudo-Voigt functions and their frequencies,

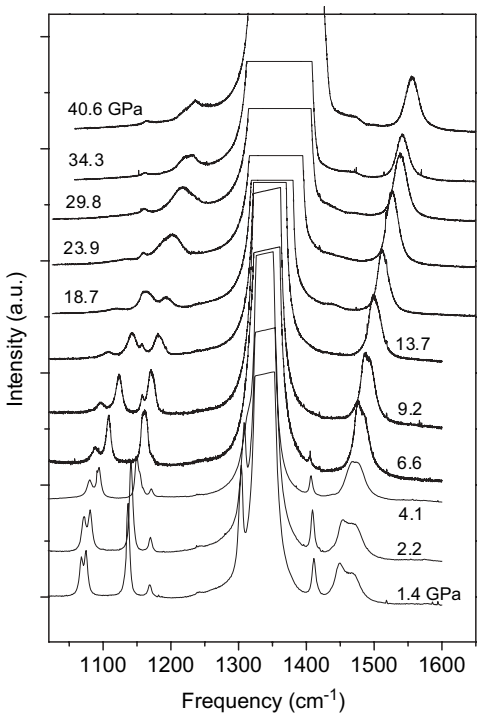

FIG. 6. Selected Raman spectra of crystalline polyethylene measured at 475 K upon pressure increase from 1.4 to 40.6 GPa. The strong band at ~1340 cm^{-1} is due to the diamond.

widths, and intensities were studied as a function of pressure. A selection of the spectra relative to the bending and C–C stretching regions measured upon compression is reported in Fig. 6. The doublet at 1065 cm^{-1} (low-pressure value) is relative to the Davydov components of the $\nu^+(0)$ chain mode, the in-phase motion between adjacent units in the chain resulting from the mixing of C–C stretching and $\widehat{CCC}$ bending motions.[29] The separation between the two components increases on compression with the lower frequency peak weakening above 6 GPa and vanishing around 20 GPa. The same peak disappears at about 10 GPa when the compression is performed at higher temperature (575 K). Therefore, on a thermal annealing basis, we can conclude that this peak is characteristic of the orthorhombic phase. Between 1100 and 1200 cm^{-1} we observe at ~1130 cm^{-1} the strong peak assigned to the $\nu^+(\pi)$ chain mode, and the weak rocking mode (γ_r) at 1170 cm^{-1}. In the region of the $\nu^+(\pi)$ chain mode a new peak appears at 3.6 GPa as a high frequency shoulder of the main peak (see Fig. 6). Also in this case a higher temperature experiment provides good hints for the assignment of this peak. As a matter of fact, during the compression at 575 K the new band is observed only when pressure is close to 9 GPa, thus suggesting its belonging to the monoclinic $P2_1m$ phase. The spectral decomposition also shows that the corresponding orthorhombic line weakens with the intensification of this peak and vanishes at 11 GPa. The weak peak at 1170 cm^{-1} is observed only up to ~8 GPa because its frequency is almost pressure independent, whereas that of the $\nu^+(\pi)$ mode increases with pressure thereby overlapping to the weak rocking peak. The peak at 1417 cm^{-1}, a wagging motion, softens with increasing pressure and it also weakens at ~3.5 GPa vanishing at about 8 GPa. With the exception of these two latter bands the frequencies of all the other Raman modes increase with pressure.

The other spectral region of interest is that relative to the scissoring mode (δ) around 1442 cm^{-1}. The peak relative to this mode overlaps to a band of comparable intensity at 1466 cm^{-1}. This latter peak is not a fundamental mode and it was assigned to a combination of two $\gamma_r(CH_2)$ (B_{1u}) infrared active modes.[29] The relative intensities of the two peaks change with pressure. Up to about 6 GPa the high frequency band at 1466 cm^{-1} intensifies. The intensification with pressure of the combination band has been interpreted on the basis of changes of the Fermi resonance interaction between the overtones and the combination bands of the infrared active rocking modes.[27,30] Above this pressure a distinct intensification of the scissoring mode at 1442 cm^{-1} occurs, whereas the overtone at 1466 cm^{-1} weakens, and vanishes at 30 GPa. The intensification of the scissoring peak could be due to the formation of the high-pressure monoclinic *A2/m* phase that appears in the XRD measurements around this pressure value. The DFT simulations are not able to provide a definite assignment of this peak to one of the two monoclinic phases (see Fig. 7). As already reported for the IR spectra a considerable hysteresis is observed in the decompression run, but the recovered spectrum is fully orthorhombic and, essentially, identical to the initial spectrum. This indicates that no irreversible changes of the crystal structure occur up to 40 GPa, thereby confirming the infrared and XRD results.

In Fig. 8 we compare the pressure shift of the infrared and Raman frequencies. The pressure behavior of the different modes are hardly sensitive to temperature and the infrared and Raman frequencies never overlap, with the only exception of a

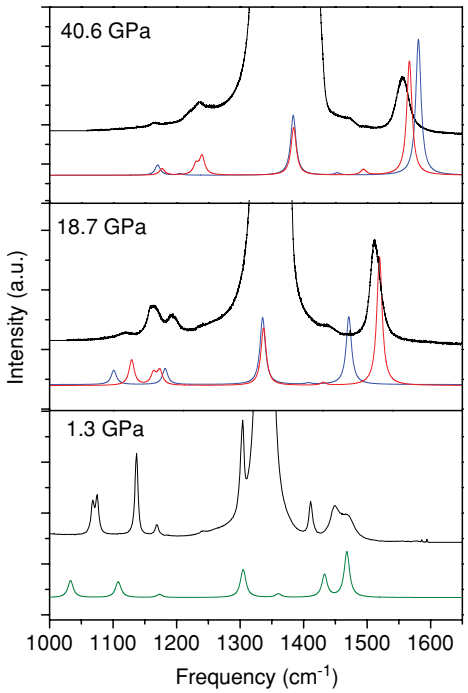

FIG. 7. Comparison between experimental (575 K) and simulated DFT (0 K) Raman spectra at three selected pressures. Green, red, and blue spectra are the calculated spectra relative to the orthorhombic (*Pnam*), monoclinic ($P2_1m$), and monoclinic (*A2/m*), respectively.

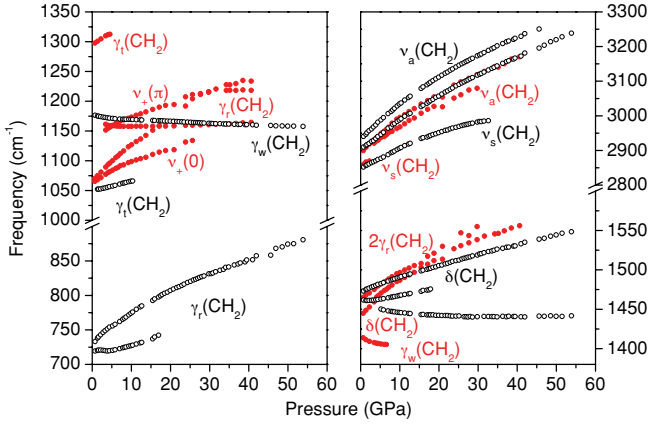

FIG. 8. Pressure shift of infrared (empty circles) and Raman (red dots) frequencies, upon compression. The vibrational modes are labeled following the assignment for the polyethylene chain from Ref. 29. γ_t, γ_r, and γ_w indicate twisting, rocking, and wagging modes, respectively, δ bending and ν stretching modes.

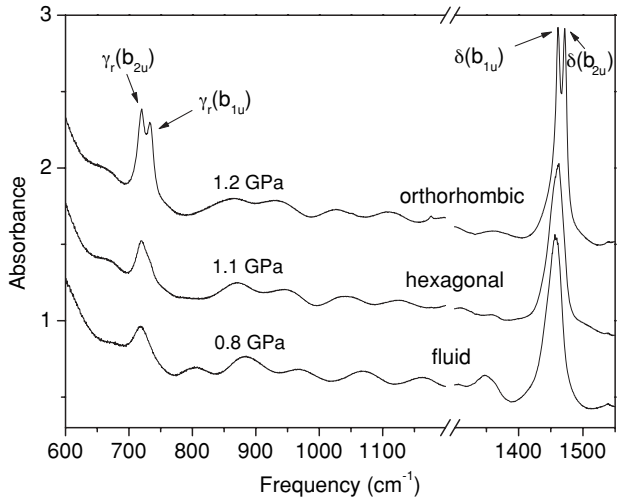

FIG. 9. Pressure evolution of the IR spectra in a decompression measurement along the 610 K isotherm showing the orthorhombic-hexagonal-liquid phase transitions.

single likely accidental coincidence in the C–H stretching region, thereby confirming that the center of inversion is always preserved as expected for phases *Pnam*, $P2_1m$, and $A2/m$. The softening of the rocking and scissoring modes at 1170 and 1440 cm^{-1}, respectively, is remarkable, thus suggesting a gradual reduction of the steric hindrance for these motions. In general, an excellent agreement is found for the frequency values measured during the decompression and compression cycles.

C. Phase diagram

The transitions from the liquid to the hexagonal and then to the orthorhombic crystal phases can be easily detected from the changes in the IR spectra. Despite the close resemblance between the spectra of the hexagonal and of the liquid phases, as expected due to the disordered nature of the crystalline hexagonal high-pressure phase, the melting of the crystal is revealed by the sudden intensification in the spectrum of interference fringes ascribable to a change of the refractive index and of the sample homogeneity (see Fig. 9). The hexagonal to orthorhombic phase transition can be clearly detected by the splitting of the hexagonal broad bands both in the rocking and in the scissoring regions as expected by group theory arguments. Our results are in good agreement with those found in the literature. The most remarkable indication of the orthorhombic-monoclinic (*Pnam*-$P2_1/m$) phase transition is the appearance in the IR spectrum of the low frequency component of the scissoring mode, at about 1430 cm^{-1}, on the low frequency side of the Davydov doublet characterizing the orthorhombic phase (see Fig. 4). The gradual strong intensification of this peak with pressure and the corresponding weakening of the orthorhombic doublet, whose low frequency component almost completely vanishes only above 20 GPa, clearly indicate a sluggish transition. This conclusion is also supported by the behavior of the lowest rocking mode component of the orthorhombic phase that completely disappears only above 17 GPa. The small enthalpy differences between the three phases reported in previous DFT calculations[4] are consistent with a coexistence scenario.

In order to draw the phase diagram reported in Fig. 10, we thereby determined the onset pressure of the orthorhombic to monoclinic (*Pnam*-$P2_1m$) phase transition, for each temperature, looking to the appearance of the low frequency peak in the scissoring spectral region during compression experiments, and its disappearance when the pressure was released. This procedure allows for the identification for each isotherm of an extended *P–T* region containing the thermodynamic *Pnam*-$P2_1/m$ phase boundary. The lack of characteristic bands of the $A2/m$ monoclinic phase does not allow for the identification of the $P2_1/m$-$A2/m$ phase transition pressure. Up to the maximum pressure reached in these experiments (~50 GPa), the spectral signatures of the lower-pressure phases were still observed, whereas the bands assigned to

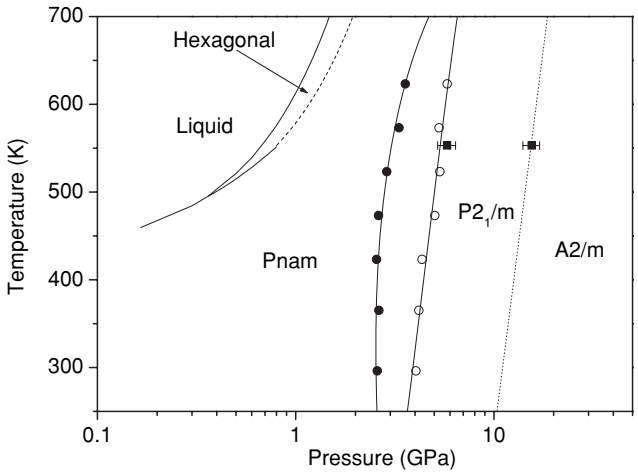

FIG. 10. Phase diagram of crystalline polyethylene after the present work. The empty dots indicate the *Pnam*-$P2_1/m$ phase transition as deduced by the appearance of the low frequency band in the IR spectra of the scissoring mode (see Fig. 4) measured upon compression. Full dots indicate the P-T values where the orthorhombic IR spectra were recovered during decompression experiments. The experimental points for the *Pnam*-$P2_1/m$ and $P2_1/m$-$A2/m$ phase transitions are from Ref. 4, whereas the dotted line is a schematic representation of the $P2_1/m$-$A2/m$ phase boundary.

the monoclinic phases persisted in decompression down to a few GPa thereby indicating extremely sluggish transformations. The stability upon decompression of the *A2/m* phase over the $P2_1/m$, reported in previous XRD studies, suggests that $P2_1/m$ is a metastable phase.[4]

IV. VIBRATIONAL COUPLING

The Davydov splitting of the modes in a crystal is due to the intermolecular forces. Because of the increase of the intermolecular forces upon increasing density, the Davydov splitting increases with pressure and the difference between the squares of the frequencies can be directly related to the intermolecular force coupling constants. Therefore, the analysis of the pressure behavior of the frequencies of Davydov components can be used to obtain information about the behavior of intermolecular couplings under pressure.

The vibrational potential for a molecular crystal Φ_v is the component of the total potential energy that depends on the fluctuations of the intramolecular bond lengths around their equilibrium values. Φ_v can be written, in the harmonic approximation, as the sum of the effective single molecule potentials and pair interaction potentials,[31–35]

$$\phi_v = \sum_i \phi(u_i, R_0) + \frac{1}{2}\sum_{i,j} G(R_{ij})u_i u_j \qquad i \neq j, \qquad (2)$$

where ϕ is the effective intramolecular potential, G is an intermolecular vibrational coupling force constant, R_{ij} is the separation between molecules i and j, R_0 is the nearest-neighbor distance, and u_i is the deviation from equilibrium separation of the nuclei for a particular molecular internal normal mode. The value of the coupling constant G for a pair of identical inequivalent molecules in the primitive cell, as it is the case with the nearest neighbor's polyethylene chains in the orthorhombic cell, can be extracted within a factor A from the experimental frequencies at each pressure as

$$G = (\omega_+^2 - \omega_-^2)A, \qquad (3)$$

where ω_+ and ω_- are the high and low frequency components of the Davydov doublet, respectively. At long distance, the force constant G is described by a negative dipole–dipole interaction term proportional to R_{ij}^{-6}. For solid hydrogen, Moshary *et al.* found an evolution of G proportional to $R_{ij}^{-7.2}$, up to 100 GPa, explaining this result with a short range correction to the intermolecular interactions.[34] A much larger value of the exponent, $R_{ij}^{-16.95}$, was instead found for the δ and α phases of solid oxygen where, also, the G resulted to be positive.[33] These findings were explained on the basis of strong short range interactions, ascribed to remarkable charge transfer process. These forces support the antiferromagnetic order in both α and δ phases.[36–38]

The G/A values were calculated from the experimental frequencies of the Davydov components in the orthorhombic *Pnam* phase for the rocking γ_r (720–731 cm^{-1}) and scissoring δ (1463–1482 cm^{-1}) IR active modes, and for the $\nu^+(0)$ (1063–1065 cm^{-1}) Raman active mode of crystalline polyethylene. The values reported in parenthesis are the frequencies of the Davydov components at ambient pressure.

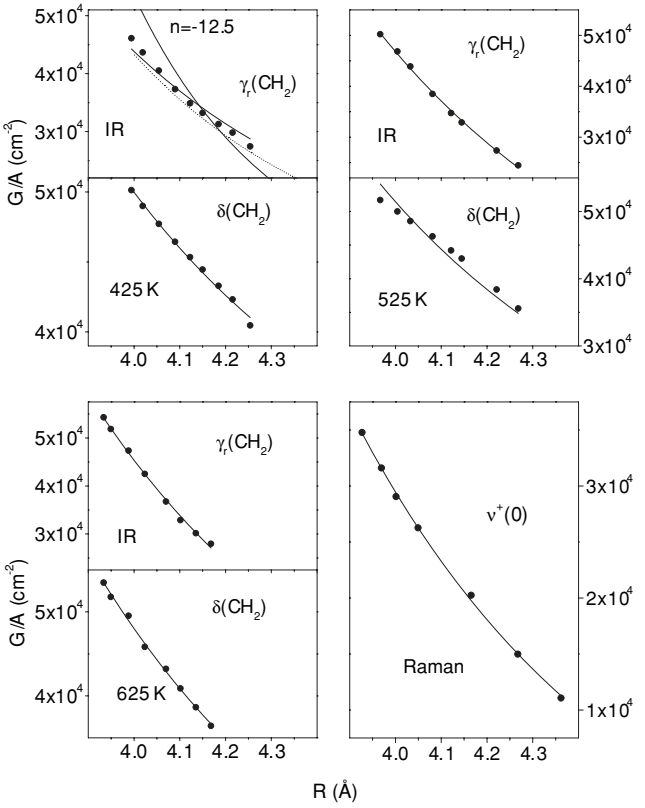

FIG. 11. Vibrational coupling constant G/A (see Eq. (2)) vs R (see Eq. (3)) for the rocking and scissoring IR active modes at three different temperatures, and for the C–C stretching Raman mode at 475 K. The R values range between 3.9 Å (~6 GPa) and 4.4 Å, being 4.5 Å; the ambient pressure value. Solid lines are drawn by using the power law reported in Eq. (5) with the n value fixed to –6. In the upper left panel the curves obtained from room temperature literature experimental[15] (dotted) and theoretical[17](full) frequencies are also reported.

The G/A values are reported in Fig. 11 as a function of the intermolecular distance R, which is equal to the distance between the axes of the two parallel polymeric chains forming the orthorhombic unit cell. R is calculated by using the equation of state reported in Ref. 4 as

$$R = \sqrt{\left(\frac{a}{2}\right)^2 + \left(\frac{b}{2}\right)^2}, \qquad (4)$$

where *a,b* are the lattice parameters of the plane perpendicular to the chain axis. The experimental values of the G/A ratio were fitted to the power law

$$y = B * R^n. \qquad (5)$$

A power law with $n = -6$, characteristic of dispersive long range dipole–dipole interactions, nicely reproduces most of the data (see Fig. 11) thus indicating the Van der Waals nature of the orthorhombic polyethylene crystal.

V. INTENSITY ANALYSIS OF THE INFRARED SPECTRA

The analysis of the pressure-induced changes of the intensity of the IR active modes can be a precious source of information about the nature of the intermolecular interactions.

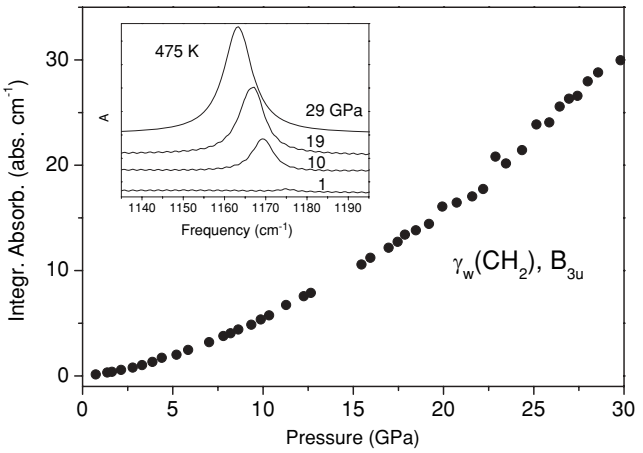

FIG. 12. Pressure evolution of the integrated absorbance of the wagging IR peak (see inset) at 475 K. The data have been obtained by fitting the band to a pseudo-Voigt profile.

In the case of polyethylene the most remarkable pressure-induced change is the anomalous intensification of the IR active wagging mode along all the isothermal compression runs as reported in Fig. 12 for the 475 K experiment. Charge transfer processes between neighboring molecules, due to the strengthening of the intermolecular interactions and leading to an increasing degree of static or dynamic ionic character of the solid, have been invoked to justify the anomalous intensification with pressure of the vibron lines in solid oxygen,[39,40] and hydrogen.[41,42] Alternative explanations for the intensification include a pressure-induced change in the relative orientation of the transition dipole moments.

For transitions that are allowed in the isolated molecule, the absorption coefficient α depends linearly on the density of molecules ρ ($\alpha = \rho\sigma$, where σ is the single molecule absorption cross section). If the material is isotropically compressed the length x of the absorbing sample is related to the density as

$$x \propto \rho^{-1/3}. \tag{6}$$

Therefore, the absorbance η, which is proportional to αx, depends on the density as

$$\eta \propto \rho\rho^{-1/3} = \rho^{2/3}. \tag{7}$$

As can be seen in Fig. 13, the integrated absorbance of the wagging mode shows, in all the isotherms, a much stronger dependence on the density ρ requiring an extra, density dependent, contribution to the cross section σ whose magnitude cannot be justified on the basis of van der Waals interactions only. DFT calculations are able to account only partially for the anomalous intensification experimentally observed for the wagging mode, giving a power coefficient n four times larger than predicted by Eq. (6), but four times smaller than that obtained from the experimental data.

Between the two processes mentioned at the beginning of this section the charge transfer process is the most likely because the dipole moment for this mode oscillates along the chain and, whereas the relative orientation of the chains is affected by the pressure increase, the dipole moment is not. This conclusion is also substantiated by the similar behavior exhibited by the scissoring mode of the monoclinic $P2_1/m$ phase. As shown in Fig. 3, this component undergoes to a strong intensification with pressure being already saturated just above 10 GPa. Unfortunately, the saturation prevents a careful analysis of the pressure evolution of its absorbance. However, in this case there are no doubts about the process causing this intensification because the primitive cell of this phase contains only one unit thus ruling out any possible change in the transition dipole moment due to a pressure tuning of the relative chain orientation.

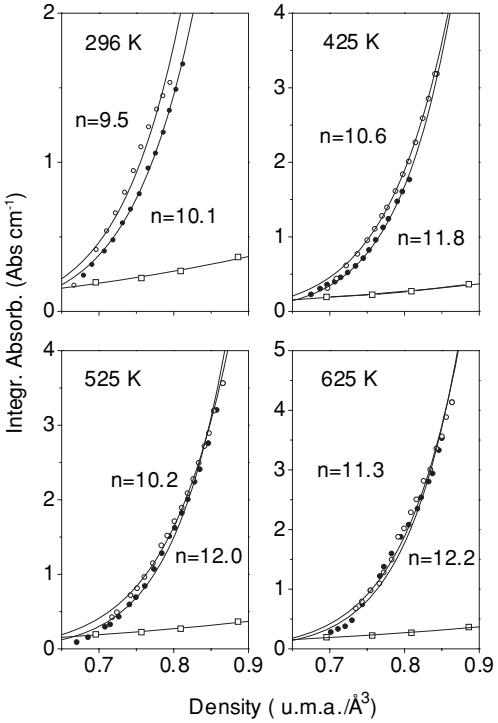

FIG. 13. Intensity of the IR active wagging mode of crystalline polyethylene as a function of density at different temperatures. Full (open) circles indicate the data upon compression (decompression) while n represents the exponent of the power law employed to fit the data (full lines, see Eq. (6)). The calculated (DFT) intensity (empty squares), scaled by an arbitrary factor, is also reported in the same density range. The full line reproducing the evolution with density is a power law with $n = 2.64$.

It has to be remarked, however, that the intensity of the wagging mode of polyethylene is anomalously low at ambient conditions, as already noticed in Refs. 43 and 44, presumably due to an accidental cancellation of terms. A third hypothesis to explain the anomalous intensification thus consists of assuming that the accidental balance leading to the low intensity of the wagging mode at ambient pressure is simply removed by the application of pressure. Any attempt to model the intensification along such lines of thought would require a calculation of the IR intensity with an accuracy that goes beyond what is currently achievable with DFT methods.

VI. CONCLUSIONS

The vibrational properties of crystalline polyethylene have been studied by FTIR, Raman, and DFT calculations along several isotherms up to 50 GPa. The peculiar vibrational signatures of the three crystal phases, $Pnam$, $P2_1/m$,

and $A2/m$ found in a previous XRD study on increasing pressure, have been identified and employed to draw a phase diagram from ambient conditions up to 50 GPa and 650 K. High-quality polyethylene crystals, prepared in the orthorhombic $Pnam$ phase through a specific annealing procedure, have been found to be chemically stable up to the most extreme conditions reached in this study, and the structural properties characterizing the polymer at ambient conditions are fully recovered in decompression. This is a relevant point in the light of the present and potential technological applications of this material. Interestingly, the higher-pressure monoclinic phase $A2/m$ is stable upon decompression down to a few GPa in agreement with a previous XRD study where the metastable character of the intermediate monoclinic $P2_1/m$ phase was proposed. Long range dispersive dipole–dipole interactions nicely model the Davydov splitting of three different modes as a function of pressure in the orthorhombic $Pnam$ crystal phase. On the contrary, charge transfer mechanisms may be the source of the anomalous intensification of the wagging and presumably of the scissoring modes in the $P2_1/m$ monoclinic phase. However, the inability of DFT calculations to reproduce the intensification and the anomalous intensity of the wagging mode at ambient pressure point to an alternative mechanism whereby pressure removes an accidental cancellation of terms in the intensity of the wagging mode at ambient conditions.

ACKNOWLEDGMENTS

Supported by the European Union FP7 G.A. No. 228334-LASERLAB EUROPE, the Italian Ministero dell'Universitá e della Ricerca Scientifica e Tecnologica (MURST), and "Firenze Hydrolab" through a grant by Ente Cassa di Risparmio di Firenze.

[1] D. Bower and W. F. Maddams, *The Vibrational Spectroscopy of Polymers* (Cambridge University Press, New York, 1989).
[2] D. C. Bassett and B. Turner, Nature **240**, 146 (1972).
[3] M. Hikosaka, S. Minomura, and T. Seto, Jpn. J. Appl. Phys. **14**, 589 (1975).
[4] L. Fontana, D. Q. Vinh, M. Santoro, R. Bini, S. Scandolo, F. A. Gorelli, and M. Hanfland Phys. Rev. B **75**, 174112 (2007).
[5] C. W. Bunn, Trans. Faraday Soc. **35**, 482 (1939).
[6] T. Ito and H. Marui, Polym. J. (Tokyo, Jpn.) **2**, 768 (1971).
[7] D. C. Bassett, S. Block, and G. J. Piermarini, J. Appl. Phys. **45**, 4146 (1974).
[8] M. Yasuniwa, R. Enoshita, and T. Takemura, Jpn. J. Appl. Phys. **15**, 1421 (1976).
[9] T. Yamamoto, H. Miyaji, and K. Asai, Jpn. J. Appl. Phys. **16**, 1891 (1977).
[10] M. Hikosaka, S. Minomura, and T. Seto, Jpn. J. Appl. Phys. **19**, 1763 (1980).
[11] M. Hikosaka, K. Tsukijima, S. Rastogi, and A. Keller, Polymer **33**, 2502 (1992).
[12] T. Seto, T. Hara, and K. Tanaka, Jpn. J. Appl. Phys. **7**, 31 (1968).
[13] K. E. Russell, B. K. Hunter, and R. D. Heyding, Polymer **38**, 1409 (1997).
[14] C.-K. Wu and M. Nicol, J. Chem. Phys. **58**, 5150 (1973).
[15] C.-K. Wu, J. Polym. Sci., Polym. Phys. Ed. **12**, 2493 (1974).
[16] W. W. Ley and H. G. Drickamer, J. Phys. Chem. **93**, 7262 (1989).
[17] D. J. Lacks, J. Phys. Chem. **99**, 14430 (1995).
[18] M. Gussoni, C. Castiglioni, and G. Zerbi, in *Spectroscopy of Advanced Materials*, edited by R. J. M. Clarck (Wiley, New York, 1991).
[19] H. K. Mao, J. Xu, and P. M. Bell, J. Geophys. Res. B **91**, 4673 (1986).
[20] L. Ciabini, F. A. Gorelli, M. Santoro, R. Bini, V. Schettino, and M. Mezouar, Phys. Rev. B **72**, 094108 (2005).
[21] R. Bini, R. Ballerini, G. Pratesi, and H. J. Jodl, Rev. Sci. Instrum. **68**, 3154 (1997).
[22] J. P. Perdew, K. Burke, and M. Ernzerhof, Phys. Rev. Lett. **77**, 3865 (1996).
[23] P. Giannozzi, Stefano Baroni, Nicola Bonini, Matteo Calandra, Roberto Car, Carlo Cavazzoni, Davide Ceresoli, Guido L Chiarotti, Matteo Cococcioni, Ismaila Dabo, Andrea Dal Corso, Stefano de Gironcoli, Stefano Fabris, Guido Fratesi, Ralph Gebauer, Uwe Gerstmann, Christos Gougoussis, Anton Kokalj, Michele Lazzeri, Layla Martin-Samos, Nicola Marzari, Francesco Mauri, Riccardo Mazzarello, Stefano Paolini, Alfredo Pasquarello, Lorenzo Paulatto, Carlo Sbraccia, Sandro Scandolo, Gabriele Sclauzero, Ari P Seitsonen, Alexander Smogunov, Paolo Umari, and Renata M Wentzcovitch, J. Phys.: Condens. Matter **21**, 395502 (2009); http://www.quantum-espresso.org.
[24] S. Baroni, S. de Gironcoli, A. Dal Corso, and P. Giannozzi, Rev. Mod. Phys. **73**, 515 (2001).
[25] M. Lazzeri and F. Mauri, Phys. Rev. Lett. **90**, 036401 (2003).
[26] S. Krimm, C. Y. Liang, and B. B. M. Sutherland, J. Chem. Phys. **25**, 549 (1956).
[27] Y. Zhao, J. Wang, Q. Cui, Z. Liu, M. Yang, and J. Shen, Polymer **31**, 1425 (1990).
[28] R. G. Snyder, Meth. Exp. Phys. A **16**, 107 (1980).
[29] S. Krimm, Fortschr. Hochpolym.-Forsch. **2**, S.51–172 (1960).
[30] C.-K. Wu and M. Nicol, Chem. Phys. Lett. **18**, 83 (1973).
[31] N. W. Ashcroft and N. D. Mermin, *Solid State Physics* (Holt, Rinehart and Winston, New York, 1976).
[32] J. Van Kranendonk, Physica **25**, 1080 (1959).
[33] F. A. Gorelli, L. Ulivi, M. Santoro, and R. Bini, Phys. Rev. B **60**, 6179 (1999).
[34] F. Moshary, N. H. Chen, and I. F. Silvera, Phys. Rev. B **48**, 12613 (1993).
[35] P. Loubeyre, R. Le Toullec, and J. P. Pinceaux, Phys. Rev. B **45**, 12844 (1992).
[36] F. A. Gorelli, M. Santoro, L. Ulivi, and R. Bini, Phys. Rev. B **62**, R3604 (2000).
[37] M. Santoro, F. A. Gorelli, L. Ulivi, R. Bini, and H. J. Jodl, Phys. Rev. B **64**, 64428 (2001).
[38] F. Gorelli, M. Santoro, R. Bini, and L. Ulivi, Phys. Rev. B **77**, 132103 (2008).
[39] F. A. Gorelli, L. Ulivi, M. Santoro, and R. Bini, Phys. Rev. Lett. **83**, 4093 (1999).
[40] L. F. Lundegaard, G. Weck, M. I. McMahon, S. Desgreniers, and P. Loubeyre, Nature **443**, 201 (2006).
[41] R. J. Hemley, Z. G. Soos, M. Hanfland, and H. K. Mao, Nature **369**, 384 (1994).
[42] Z. G. Soos, J. H. Eggert, R. J. Hemley, M. Hanfland, and H. K. Mao, Chem. Phys. **200**, 23 (1995).
[43] O. Theimer, J. Chem. Phys. **27**, 1041 (1957).
[44] J. Rud Nielsen and R. F. Holland, J. Mol. Spectr. **4**, 488 (1960).